Chemical Physics 88 (1984) 309–313
North-Holland, Amsterdam

MEASUREMENT OF ABSORPTION CROSS SECTIONS IN THE LONG-WAVELENGTH REGION OF THE S_0–S_1 ABSORPTION BAND OF DYES

A. PENZKOFER and P. SPERBER

Naturwissenschaftliche Fakultät II – Physik, Universität Regensburg, 8400 Regensburg, FRG

Received 20 February 1984

In the long-wavelength region of the S_0–S_1 absorption band of dyes only a fraction of molecules takes part in the absorption process. The absorption cross section of the molecules involved is deduced from non-linear transmission measurements with picosecond light pulses. The absorption cross sections $\sigma_A(\nu_L)$ (ν_L is the ruby-laser frequency) of 1,1′-diethyl-2,4′-carbocyanine iodide in methanol and oxazine 1 perchlorate in ethanol are determined.

1. Introduction

All dye molecules contribute to the S_0–S_1 absorption spectrum around the absorption peak and at the short-wavelength side. The absorption cross section σ_A is easily derived from transmission measurements with a spectrophotometer ($\sigma_A = \alpha_A/N_0$, $\alpha_A = -\ln(T_0)/l$, where α_A is the absorption coefficient, N_0 the total number density of dye molecules, T_0 the small signal transmission and l the sample length). In the long-wavelength region of the S_0–S_1 absorption band only a fraction of molecules takes part in the absorption process (thermally excited molecules and inhomogeneously shifted molecules) and the absorption cross section of the molecules involved can no longer be determined with a spectrophotometer.

The absorption cross section in this long-wavelength region ($\nu < \nu_{F,m}$; $\nu_{F,m}$ is the frequency of peak fluorescence emission) is generally derived from fluorescence measurements [1–3]. Here a non-linear transmission technique with picosecond light pulses is described for the measurement of the absorption cross sections. The technique is applied to measure the absorption cross section $\sigma_A(\nu_L)$ of two dyes, dicyanine (1,1′-diethyl-2,4′-carbocyanine iodide, DCI′) [4–6] in methanol and oxazine 1 perchlorate [7,8] in ethanol, at the ruby-laser frequency ν_L. The results of the bleaching technique are compared with the results of the fluorescence technique.

The non-linear transmission technique with picosecond pulses as it is described in the following is limited to dyes with negligible singlet–triplet absorption cross sections and with intersystem-crossing rates small compared to the inverse picosecond pulse duration. Furthermore the dyes should completely dissolve to monomers.

2. Theory

Fig. 1a shows a singlet potential-energy diagram of a dye molecule. The transitions of peak S_0–S_1 absorption at $\nu_{A,m}$, of peak S_1–S_0 emission at $\nu_{F,m}$ and the most probable transition of laser light at ν_L ($\nu_L < \nu_{F,m}$) are indicated. The rovibrational levels of the ground state are thermally populated. The S_0–S_1 frequency spacing is inhomogeneously broadened. A multitude of transitions between S_0 and S_1 rovibrational levels are possible at a fixed laser frequency.

Fig. 1b indicates the absorption and emission cross sections. The apparent absorption cross section $\bar{\sigma}_A(\nu) = \alpha_A(\nu)/N_0$ and apparent emission cross section $\bar{\sigma}_E(\nu) = \alpha_E(\nu)/N_0$ (α_E is the stimulated emission coefficient) are given by the solid curves [3,9]. The absorption cross section of really inter-

0301-0104/84/$03.00

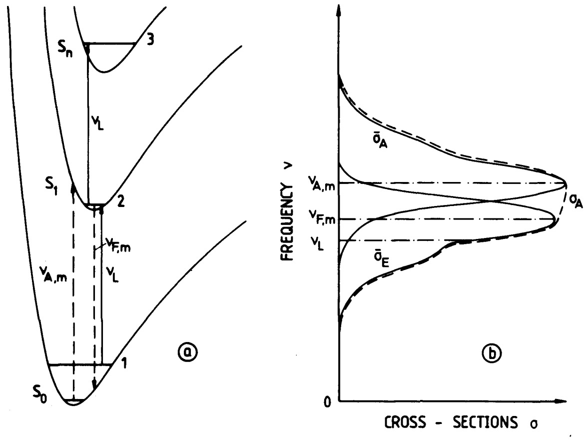

Fig. 1. (a) Potential energy diagram. (b) Apparent S_0–S_1 absorption and stimulated emission cross sections (solid curves) together with real absorption cross-section spectrum of interacting molecules (dashed curve).

acting molecules versus wavelength is indicated by the dashed curve. For $\nu \geqslant \nu_{A,m}$ $\sigma_A(\nu) \approx \bar\sigma_A(\nu)$ since all molecules (thermally excited and inhomogeneously broadened) take part in the absorption with approximately equal strength. For $\nu \leqslant \nu_{A,m}$ the apparent absorption cross section $\bar\sigma_A(\nu)$ reduces because only a tail of thermally excited and inhomogeneously broadened molecules overcomes the energy separation to the lowest states in the S_1 band and can take part in the absorption process. In the case of $\nu \leqslant \nu_{F,m}$ the transitions from the thermally excited and inhomogeneously shifted moiety in the S_0 band to the S_1 band are identical to the fluorescence transitions from the thermally relaxed S_1 band to the S_0 band. Therefore, the absorption cross section of the really interacting molecules in the long-wavelength tail ($\nu \leqslant \nu_{F,m}$) becomes equal to the apparent stimulated emission cross section $\bar\sigma_E(\nu)$, i.e. $\sigma_A(\nu) = \bar\sigma_E(\nu)$. All thermally relaxed molecules in the S_1 state have approximately the same stimulated emission cross section for $\nu \leqslant \nu_{F,m}$, i.e. $\sigma_E(\nu) = \bar\sigma_E(\nu)$. In the case of $\nu > \nu_{F,m}$ only a high-frequency tail of excited molecules in the S_1 state can emit and the high-frequency tail of $\bar\sigma_E(\nu)$ results $[\bar\sigma_E(\nu) < \sigma_E(\nu)]$.

In early studies [10] the S_0–S_1 absorption band was considered to consist of an inhomogeneous distribution of homogeneously broadened lines with only one S_0–S_1 transition level per molecule. This model led to enormously large absorption cross sections of $\sigma_A(\nu) = \alpha_A(\nu)\Delta\nu_h/N_0\Delta\nu_{inh}$ where $\Delta\nu_h$ and $\Delta\nu_{inh}$ are the homogeneous and inhomogeneous linewidths, respectively.

The effective stimulated emission cross section $\bar\sigma_E(\tilde\nu)$ depends on the radiative lifetime τ_{rad} and the spectral shape $E(\tilde\nu)$ (quantum distribution $\int E(\tilde\nu)\,d\tilde\nu = 1$) of the fluorescence signal [1]:

$$\bar\sigma_E(\tilde\nu) = E(\tilde\nu)/8\pi\eta_F^2 c\tilde\nu^2\tau_{rad}, \tag{1}$$

where c is the vacuum light velocity, η_F the mean refractive index of the solution in the fluorescence region, $\tilde\nu = \nu/c = 1/\lambda$ is the wavenumber in cm^{-1}. The radiative lifetime τ_{rad} may be calculated by use of the Strickler–Berg formula [2],

$$\tau_{rad}^{-1} = \frac{8\pi\eta_F^3 c}{\eta_A}\,\frac{\int E(\tilde\nu)\tilde\nu^{-1}\,d\tilde\nu}{\int E(\tilde\nu)\tilde\nu^{-4}\,d\tilde\nu}\int\bar\sigma_A(\tilde\nu)\tilde\nu^{-1}\,d\tilde\nu, \tag{2}$$

where η_A is the mean refractive index of the solution in the absorption region, or by measuring the fluorescing lifetime τ_F and the fluorescence quantum efficiency q_F,

$$\tau_{rad} = \tau_F/q_F. \tag{3}$$

The theory of non-linear light transmission through dyes in the long-wavelength absorption region follows exactly the theory of ref. [3] where the possible S_0–S_1 transitions are comprised in a two-level system (levels 1 and 2 of fig. 1a, for details see ref. [3]). $\sigma_A(\nu_L)$ is obtained by comparing experimental energy-transmission data with calculated energy-transmission curves $T_E(I_{0L}, \Delta t_L)$. The initial condition for the interacting molecules is $N_1(\theta, r, t' = -\infty, z) = \alpha_A(\nu_L)/\sigma_A(\nu_L) = -\ln(T_0)/l\sigma_A(\nu_L)$ which involves the parameter $\sigma_A(\nu_L)$ to be determined. The energy transmission depends on the pulse parameters I_{0L} (peak intensity), $s(r', t')$ (temporal and spatial pulse shape, gaussian shape used in calculations), Δt_L (pulse duration) and on the dye parameters $\sigma_A(\nu_L)$, τ_F (fluorescence lifetime), T_3 (spectral cross-relaxation time), σ_{ex} (excited-state absorption cross section), τ_{ex} (relaxation time of levels populated by excited-state absorption) and τ_{or} (reorientation time of transition dipole moments).

The pulse parameters are measured in the experiments. The dye parameters $\sigma_A(\nu_L)$ and $\sigma_{ex}(\nu_L)$ are determined from the energy-transmission measurements. $\sigma_{ex}(\nu_L)$ is obtained by fitting the calculated energy-transmission curves at high input intensities to the energy-transmission data. It is given by

$$\sigma_{ex}(\nu_L) = -\kappa \ln[T_E(I_{0L} \to \infty)]\, \sigma_A(\nu_L)/\alpha_A(\nu_L),$$

with κ close to one [3]. It should be small compared to $\sigma_A(\nu_L)$. For $\sigma_{ex}(\nu_L)$ comparable to $\sigma_A(\nu_L)$ the described picosecond bleaching technique cannot be used. The S_1-state lifetime τ_F has to be measured separately, for example by streak camera measurements of the fluorescence decay after picosecond pulse excitation or by absorption-recovery analysis with picosecond pump and probe techniques (methods reviewed in refs. [9,11,12]). The spectral cross-relaxation time T_3 describes refilling of depopulated levels in the S_0 band by thermalisation and redistribution within the inhomogeneous profile [3]. For $T_3 \gg \Delta t_L$ no refilling of states in the interaction region of the S_0 band occurs. Complete bleaching is observed when half of the initially present molecules is transferred to the S_1 state. The level populations at complete bleaching are $N_1 = N_2 = \frac{1}{2}N_1(t' = -\infty)$. In the case of $T_3 \ll \Delta t_L$ the involved states in the S_0-band are refilled from the S_0 reservoir and complete bleaching is observed for the level populations $N_1 = N_2 \approx N_1(t' = -\infty)$. A pulse energy of a factor of two higher is necessary for $T_3 \ll \Delta t_L$ compared to $T_3 \gg \Delta t_L$ in order to achieve the same bleaching effect. In our calculations we assumed $T_3 \ll \Delta t_L$. The reported σ_L values would be a factor of two smaller for $T_3 \gg \Delta t_L$. The S_n state populated by excited-state absorption is assumed to relax to the S_1 state with a decay time τ_{ex} which is generally in the subpicosecond region [13–15]. $\tau_{ex} = 10^{-13}$ s is used in the calculations. In some dye molecules S_2-state lifetimes in the picosecond [16–22] and sub-nanosecond-to-nanosecond region [23,24] have been found. The slight influence of τ_{ex} on σ_A determination is discussed below.

3. Experiments

The absorption cross sections of the dyes dicyanine in methanol and oxazine 1 in ethanol have been measured. For the fluorescence technique [eqs. (1)–(3)] the S_0–S_1 absorption spectra were measured with a conventional spectrophotometer [$\bar{\sigma}_A(\tilde{\nu})$] and the fluorescence spectral shapes $E(\tilde{\nu})$ were obtained by He–Ne-laser excitation and fluorescence detection at right angles to the excitation beam with a spectrometer and an optical multichannel analyser.

The bleaching technique was performed with single picosecond pulses from a mode-locked ruby laser. The energy transmission through the dyes was measured with photodetectors. The input-pulse peak intensity was determined by two-photon transmission measurements through a CdS crystal [25] (the error in the single-shot peak-intensity detection is ≈ ±10%). The ruby-laser pulse duration was determined by two-photon fluorescence detection [26].

4. Results

The S_0–S_1 absorption spectra $\bar{\sigma}_A(\nu)$ and the fluorescence spectra $\bar{\sigma}_E(\nu)$ of solutions of dicyanine in methanol and oxazine 1 in ethanol are shown in figs. 2 and 3, respectively. The absorption cross sections at the ruby-laser frequency are $\sigma_A(\nu_L) = \bar{\sigma}_E(\nu_L) = (3.1 \pm 0.3) \times 10^{-16}$ cm^2 for dicyanine and $(2.5 \pm 0.3) \times 10^{-16}$ cm^2 for oxazine 1.

The energy-transmission data are depicted in

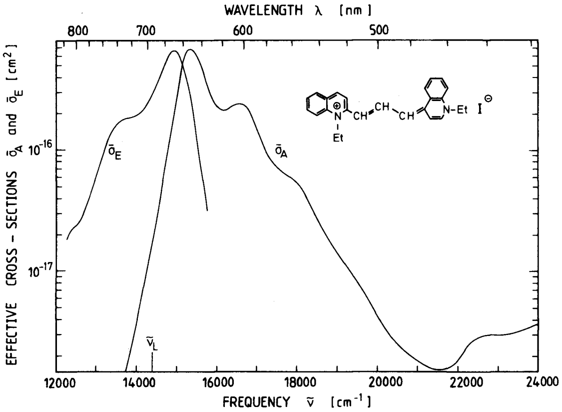

Fig. 2. Absorption and fluorescence spectrum of dicyanine (DCI′) in methanol.

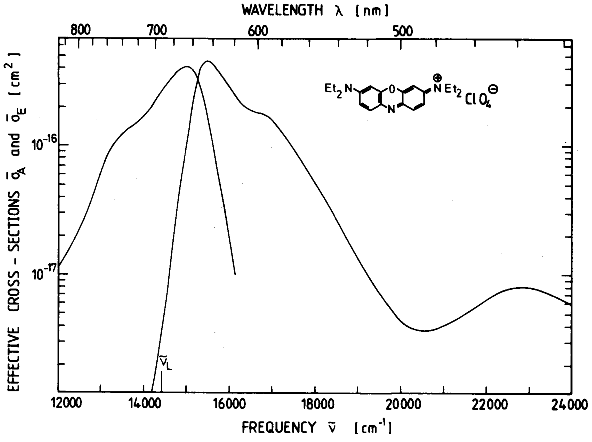

Fig. 3. Absorption and fluorescence spectrum of oxazine 1 perchlorate in ethanol.

figs. 4a and 4b. The curves are calculated with the dye and pulse parameters listed in table 1. σ_A and σ_{ex} are varied for the different curves. The best-fit values to the experimental points, σ_A(dicyanine) = $(3 \pm 0.4) \times 10^{-16}$ cm^2 and σ_A(oxazine 1) = $(2.2 \pm 0.4) \times 10^{-16}$ cm^2, are included in table 1. Each data point represents an average over about ten shots. The error bars indicate the standard deviation. The influence of the S_n-S_1 decay time τ_{ex} on the measurement of the long-wavelength absorption cross section was analysed for the dyes studied. The influence is found to be small. For example, if $\tau_{ex} = 10$ ps is assumed instead of $\tau_{ex} = 0.1$ ps the best-fitting σ_A and σ_{ex} values change by less than 10% to σ_A(dicyanine) = 3.0×10^{-16} cm^2, σ_{ex}(dicyanine) = 9.1×10^{-17} cm^2, σ_A(oxazine 1) = 2.4×10^{-16} cm^2 and σ_{ex}(oxazine 1) = 2.2×10^{-17} cm^2. The $\sigma_A(\nu_L)$ data determined by fluorescence techniques $[\bar{\sigma}_E(\nu_L)]$ and by the bleaching technique agree quite well.

In the case of dicyanine $\tau_F \ll \Delta t_L$ and the energy transmission is strongly intensity dependent [9,27]. For oxazine 1 we have $\tau_F \gg \Delta t_L$ so that the energy transmission is determined by the pulse energy [9,28]. In both cases the measurement of $T_E(I_{0L}, \Delta t_L)$ allows the determination of the long-wavelength absorption cross section σ_A.

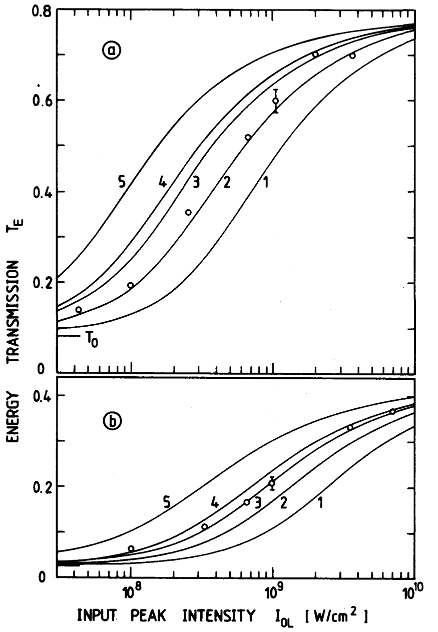

Fig. 4. Energy transmission of mode-locked ruby-laser pulses versus input peak intensity. (a) Oxazine 1 in ethanol. Curves are calculated for $\sigma_{ex} = 0.106\ \sigma_A$. 1: $\sigma_A = 1 \times 10^{-16}$ cm^2; 2: $\sigma_A = 2 \times 10^{-16}$ cm^2; 3: $\sigma_A = 3 \times 10^{-16}$ cm^2; 4: $\sigma_A = 4 \times 10^{-16}$ cm^2; 5: $\sigma_A = 8 \times 10^{-16}$ cm^2. (b) Dicyanine in methanol. Curves for $\sigma_{ex} = 0.288\ \sigma_A$. 1: $\sigma_A = 1 \times 10^{-16}$ cm^2; 2: $\sigma_A = 2 \times 10^{-16}$ cm^2; 3: $\sigma_A = 3 \times 10^{-16}$ cm^2; 4: $\sigma_A = 4 \times 10^{-16}$ cm^2; 5: $\sigma_A = 8 \times 10^{-16}$ cm^2.

Table 1
Parameters used and results

Parameter	Dicyanine	Oxazine 1
time constants (ps)		
τ_F	9.5 $^{a)}$	1020 $^{b)}$
T_3 $^{c)}$	1	1
τ_{ex} $^{c)}$	0.1	0.1
τ_{or}	140 $^{d)}$	200 $^{e)}$
τ_{rad} $^{f)}$	4600	5200
cross sections (cm^2)		
$\bar{\sigma}_A(\nu_L)$ $^{f)}$	1.4×10^{-17}	3.8×10^{-18}
$\bar{\sigma}_E(\nu_L)$ $^{f)}$	$(3.1 \pm 0.3) \times 10^{-16}$	$(2.5 \pm 0.3) \times 10^{-16}$
$\sigma_A(\nu_L)$ $^{f)}$	$(3.0 \pm 0.4) \times 10^{-16}$	$(2.2 \pm 0.4) \times 10^{-16}$
$\sigma_{ex}(\nu_L)$ $^{f)}$	$(8.6 \pm 1) \times 10^{-17}$	$(2.3 \pm 0.4) \times 10^{-17}$
laser data		
$\tilde{\nu}_L$ (cm^{-1})	14403	14403
$s(t, r)$	gaussian	gaussian
Δt_L (ps)	30	25

a) Ref. [6]. b) Ref. [8]. c) Assumed. d) Ref. [29].
e) Estimated from the Debye–Stokes–Einstein hydrodynamic model [30].
f) This work.

5. Conclusions

A picosecond pulse bleaching technique has been described for the measurement of the absorption cross section of molecules absorbing at the long-wavelength side of the S_0–S_1 absorption band. The technique is applicable if the excited-state absorption σ_{ex} is smaller than the absorption cross section σ_A and the S_1-state lifetime is known from other measurements. The excited-state absorption cross section and the ground-state absorption cross section are determined. The method is applicable independent of the duration of the S_1-state lifetime compared to the picosecond pump pulse duration.

Acknowledgement

The authors thank Dr. W. Blau and Mr. W. Dankesreiter for preliminarily measurements and the Rechenzentrum of the University for disposal of computer time. They acknowledge financial support by the Deutsche Forschungsgemeinschaft.

References

[1] O.G. Peterson, J.P. Webb, W.C. McColgin and J.H. Eberly, J. Appl. Phys. 42 (1971) 1917.
[2] S.J. Strickler and R.A. Berg, J. Chem. Phys. 37 (1962) 814.
[3] W. Blau, W. Dankesreiter and A. Penzkofer, Chem. Phys. 85 (1984) 473.
[4] M.W. McGeoch, Opt. Commun. 7 (1973) 116.
[5] E.G. Arthurs, D.J. Bradley, P.N. Puntambekar, I.S. Ruddock and T.J. Glynn, Opt. Commun. 12 (1974) 360.
[6] V. Sundström and T. Gillbro, Chem. Phys. 61 (1981) 257.
[7] K.H. Drexhage, in: Topics in applied physics, Vol. 1, Dye lasers, 2nd. Ed., ed. F.P. Schäfer (Springer, Berlin, 1977) p. 144.
[8] G.S. Beddard, T. Doust and G. Porter, Chem. Phys. 61 (1981) 17.
[9] A. Penzkofer and W. Blau, Opt. Quantum Electron. 15 (1983) 325.
[10] M. Hercher, Appl. Opt. 6 (1967) 947.
[11] S.L. Shapiro, ed., in: Topics of applied physics, Vol. 18. Ultrashort light pulses (Springer, Berlin, 1977).
[12] A.G. Doukas, J. Buchert and R.R. Alfano, in: Biological events probed by ultrafast laser spectroscopy, ed. R.R. Alfano (Academic Press, New York, 1982) p. 387.
[13] W. Falkenstein, A. Penzkofer and W. Kaiser, Opt. Commun. 27 (1978) 151.
[14] C.V. Shank, E.P. Ippen and O. Teschke, Chem. Phys. Letters 45 (1977) 291.
[15] M. Kasha, Discussions Faraday Soc. 9 (1950) 14.
[16] H. Tashiro and T. Yajima, Chem. Phys. Letters 42 (1976) 553.
[17] H. Schüller and H. Puell, Opt. Commun. 3 (1971) 352.
[18] C. Lin and A. Dienes, Opt. Commun. 9 (1973) 21.
[19] J.R. Huber and M. Mahaney, Chem. Phys. Letters 30 (1975) 410.
[20] R.W. Anderson, R.M. Hochstrasser and H.J. Pownall, Chem. Phys. Letters 43 (1976) 224.
[21] T. Kobayashi and S. Nagakura, Chem. Phys. 23 (1977) 153.
[22] K. Kasatani, M. Kawasaki and H. Sato, Chem. Phys. 83 (1984) 461.
[23] M. Maciejewski and P.P. Steer, Chem. Phys. Letters 100 (1983) 540.
[24] M. Beer and H.C. Longuet-Higgins, J. Chem. Phys. 32 (1955) 1930.
[25] W. Blau and A. Penzkofer, Opt. Commun. 36 (1981) 419.
[26] J.A. Giordmaine, P.M. Rentzepis, S.L. Shapiro and K.W. Wecht, Appl. Phys. Letters 11 (1967) 216.
[27] W. Blau, R. Reber and A. Penzkofer, Opt. Commun. 43 (1982) 210.
[28] G. Grönninger and A. Penzkofer, Opt. Quantum Electron. 16 (1984) 225.
[29] D. Waldeck, A.J. Cross, D.B. McDonald and G.R. Fleming, J. Chem. Phys. 74 (1981) 3381.
[30] T.J. Chuang and K.B. Eisenthal, Chem. Phys. Letters 11 (1971) 368.